

# Spectroscopic evidence for SN 2010ma associated with GRB 101219B <sup>1</sup>

M. Sparre<sup>1</sup>, J. Sollerman<sup>2</sup>, J. P. U. Fynbo<sup>1</sup>, D. Malesani<sup>1</sup>, P. Goldoni<sup>3,4</sup>, A. de Ugarte Postigo<sup>1</sup>, S. Covino<sup>5</sup>, V. D’Elia<sup>6,7</sup>, H. Flores<sup>8</sup>, F. Hammer<sup>8</sup>, J. Hjorth<sup>1</sup>, P. Jakobsson<sup>9</sup>, L. Kaper<sup>10</sup>, G. Leloudas<sup>1</sup>, A. J. Levan<sup>11</sup>, B. Milvang-Jensen<sup>1</sup>, S. Schulze<sup>9</sup>, G. Tagliaferri<sup>5</sup>, N. R. Tanvir<sup>12</sup>, D. J. Watson<sup>1</sup>, K. Wiersema<sup>12</sup>, R. A. M. J. Wijers<sup>10</sup>

## ABSTRACT

We report on the spectroscopic detection of supernova SN 2010ma associated with the long gamma-ray burst GRB 101219B. We observed the optical counterpart of the GRB on three nights with the X-shooter spectrograph at the VLT. From weak absorption lines, we measure a redshift of  $z = 0.55$ . The first epoch UV–near-infrared afterglow spectrum, taken 11.6 hr after the burst, is well fit by a power law consistent with the slope of the X-ray spectrum. The second and third epoch spectra (obtained 16.4 and 36.7 days after the burst), however, display clear bumps closely resembling those of the broad-lined type-Ic SN 1998bw if placed at  $z = 0.55$ . Apart from demonstrating that spectroscopic SN signatures can be observed for GRBs at these large distances, our discovery makes a step forward in establishing a general connection between GRBs and SNe. In fact, unlike most previous unambiguous GRB-associated SNe, GRB 101219B has a large gamma-ray energy ( $E_{\text{iso}} = 4.2 \times 10^{51}$  erg), a bright afterglow, and obeys the “Amati” relation, thus being fully consistent with the cosmological population of GRBs.

*Subject headings:* Supernovae: individual: SN2010ma, Gamma-ray burst: individual: GRB 101219B, Gamma-ray burst: general.

## 1. Introduction

Within the last 13 years a connection between two of the most energetic phenomena in our uni-

of Amsterdam, Science Park 904, 1098 XH Amsterdam, The Netherlands

<sup>11</sup>Department of Physics, University of Warwick, Coventry, CV4 7AL, UK

<sup>12</sup>Department of Physics and Astronomy, University of Leicester, University Road, Leicester, LE1 7RH, UK

<sup>1</sup>Based on observations collected at the European Organisation for Astronomical Research in the Southern Hemisphere, Chile, under program 086.A-0073(B). Also based on observations obtained at the Gemini Observatory, which is operated by the Association of Universities for Research in Astronomy, Inc., under a cooperative agreement with the NSF on behalf of the Gemini partnership: the National Science Foundation (United States), the Science and Technology Facilities Council (United Kingdom), the National Research Council (Canada), CONICYT (Chile), the Australian Research Council (Australia), Ministério da Ciência e Tecnologia (Brazil) and Ministerio de Ciencia, Tecnología e Innovación Productiva (Argentina)

<sup>1</sup>Dark Cosmology Centre, Niels Bohr Institute, University of Copenhagen, Juliane Maries Vej 30, 2100 Copenhagen, Denmark

<sup>2</sup>Oskar Klein Centre, Department of Astronomy, AlbaNova, Stockholm University, 106 91 Stockholm, Sweden

<sup>3</sup>Laboratoire Astroparticule et Cosmologie, 10 rue A. Domon et L. Duquet, 75205 Paris Cedex 13, France

<sup>4</sup>DSM/IRFU/Service d’Astrophysique, CEA/Saclay, 91191, Gif-sur-Yvette, France

<sup>5</sup>INAF, Osservatorio Astronomico di Brera, via E. Bianchi 46, 23807 Merate (LC), Italy

<sup>6</sup>INAF, Osservatorio Astronomico di Roma, Via Frascati 33, I-00040 Monteporzio Catone, Italy

<sup>7</sup>ASI, Science Data Center, via Galileo Galilei, I-00044 Frascati, Italy

<sup>8</sup>Laboratoire GEPI, Observatoire de Paris, CNRS-UMR8111, Univ. Paris-Diderot 5 place Jules Janssen, 92195 Meudon France

<sup>9</sup>Centre for Astrophysics and Cosmology, Science Institute, University of Iceland, Dunhagi 5, IS-107 Reykjavik, Iceland

<sup>10</sup>Astronomical Institute “Anton Pannekoek”, University

verse, long-duration gamma-ray bursts (GRBs,  $T_{90} > 2$  s; Kouveliotou et al. 1993) and core-collapse supernovae (SNe), has been established (e.g., Woosley & Bloom 2006).

The first SN associated with a GRB was reported by Galama et al. (1998), who found the extremely luminous SN 1998bw to be associated with GRB 980425. Subsequently, several other GRB-SNe were found, and a few of these have also been spectroscopically confirmed, most prominently GRB 030329 (Hjorth et al. 2003; Stanek et al. 2003), GRB 031203 (Malesani et al. 2004), GRB 060218 (Pian et al. 2006; Sollerman et al. 2006), and GRB 100316D (Starling et al. 2011; Bufano et al. 2011; Chornock et al. 2010; Cano et al. 2011). All these SNe are broad-lined type Ic; they lack lines from hydrogen and helium in their spectra and have broader lines than typical core-collapse SNe.

Most of these spectroscopic SN-associated GRBs are low-luminosity GRBs for which the emitted energies in the  $\gamma$ -ray band are in the range  $10^{48}$ – $10^{50}$  erg (e.g., Amati et al. 2007; Nysewander et al. 2009), which is 2–4 orders of magnitude smaller than for typical GRBs detected at larger distances. They also had comparably fainter or undetected optical and X-ray afterglows, and did not always obey the  $E_{\text{peak}}-E_{\text{iso}}$  correlation (Amati et al. 2007). The only well-known exception is GRB 030329 at  $z = 0.167$ . It is therefore crucial to test whether the SN-GRB connection holds in general for high-redshift, high-luminosity GRBs. To date, evidence in this direction is provided by the photometric detection of SN-like bumps in the late-time light curves of several GRBs (e.g., Zeh et al. 2004; Fynbo et al. 2004; Tanvir et al. 2010; Cano et al. 2011). Spectroscopy was also obtained in a few cases (e.g., Garnavich et al. 2003; Della Valle et al. 2003, 2006, 2008), although the contamination from the host galaxy and the faintness of the targets makes it difficult to reach firm conclusions in some of these cases.

GRB 101219B was detected by the *Swift* Burst Alert Telescope (BAT) on 2010 December 19 at 16:27:53 UT. Its afterglow was promptly detected by *Swift* both in the X-ray and UV/optical bands (Gelbord et al. 2010a). The GRB was observed to have a duration of  $T_{90} = 34 \pm 4$  s in the 15–150 keV band (Cummings et al. 2010). It was

also observed by *Fermi*/GBM, where a duration of  $T_{90} = 51 \pm 2$  s was determined in the 10–1000 keV band (van der Horst et al. 2010). The spectrum of the prompt emission as measured by GBM is well fitted by the Band model with a peak energy at  $70 \pm 8$  keV. The fluence measured by GBM is  $(5.5 \pm 0.4) \times 10^{-6}$  erg cm $^{-2}$  (10–1000 keV). Given a redshift of 0.55 (see § 3.1), this corresponds to an isotropic equivalent energy  $E_{\text{iso}} = 4.2 \times 10^{51}$  erg.

In this *Letter* we report on the spectroscopic detection of a SN associated with GRB 101219B. In § 2 we describe our observations, in § 3 we present the redshift measurement and the detection of the SN. Finally, in § 4 we offer a discussion of how this GRB-SN fits in our current understanding of the GRB-SN connection.

For the cosmological calculations we assume a  $\Lambda$ CDM-universe with  $h_0 = 0.71$ ,  $\Omega_m = 0.27$ , and  $\Omega_\Lambda = 0.73$ .

## 2. Observations and data reduction

We observed the afterglow of GRB 101219B using the X-shooter spectrograph (D’Odorico et al. 2006; Vernet et al. 2010) mounted at UT2 of the ESO-VLT on Cerro Paranal. X-shooter is an echelle spectrograph with three arms covering the full spectral range from the atmospheric cut-off around 3000 Å to the *K* band (24,800 Å).

An overview of the observations is given in Table 1. For the UVB, VIS and NIR arms, slit-widths of 1''0, 0''9, and 0''9, respectively, were used. The binning was  $1 \times 2$  in all UVB and VIS exposures, and NIR-exposures were unbinned. The slit was always aligned along the parallactic angle, and the instrument has an atmospheric dispersion corrector for the UVB and VIS arms.

We processed the spectra using the X-shooter data reduction pipeline (Goldoni et al. 2006; Modigliani et al. 2010) version 1.2.2. The pipeline performs all the standard reductions required to obtain flux calibrated echelle spectra.

All three spectra were corrected for Galactic extinction using  $R_V = 3.1$  and the prescription from Cardelli et al. (1989) with  $E(B - V) = 0.02$  mag (Schlegel et al. 1998). The spectra were reduced in staring mode and flux-calibrated using observations of the spectrophotometric standard star LTT 3218 (Hamuy et al. 1993). We performed photom-

Table 1: Overview of the X-shooter observations. The  $R$ -band magnitudes were derived from the acquisition images.

	Epoch 1	Epoch 2	Epoch 3
Mean time (UT)	2010 Dec 20.17	2011 Jan 5.09	2011 Jan 25.55
Time since GRB	11.6 hr	16.4 days	36.9 days
Exposure time (s)	4800	7200	7200
Seeing (")	0.93–1.11	0.78–0.85	0.89–0.97
Airmass	1.56–2.60	1.19–1.99	1.43–2.11
$R$ magnitude	$19.8 \pm 0.2$	$22.7 \pm 0.2$	$> 22.7$

etry of the transient on the  $R$ -band acquisition images of X-shooter (Table 1). Although our photometry could be calibrated only relative to two faint USNO stars, our results are fully consistent with nearly simultaneous measurements obtained by GROND (Olivares et al. 2010). We therefore decided to scale our spectra in order to match the GROND photometry. A relatively large correction (a factor of 2.0) was needed for the first-epoch spectrum, probably due to the high airmass of the observation. The second spectrum was also scaled to the GROND photometry (Olivares et al. 2011), but only a small correction (5%) was necessary.

For the third epoch, we compared our spectrum with late-time *ugri* imaging secured by us with the Gemini South telescope equipped with GMOS on Jan 29 (*u*) and on Jan 30 (*gri*), about 40 days after the BAT trigger. The flux in the spectrum matches well our photometric measurements.

### 3. Results

#### 3.1. Redshift measurement

The first epoch spectrum is characterized by a power-law spectral shape typical for GRB afterglows. Only weak absorption lines are present, which makes it difficult to firmly determine the spectroscopic redshift. We tentatively reported a redshift of  $z = 0.5519$  (de Ugarte Postigo et al. 2011) mainly based on the Mg II 2796, 2803 Å doublet. We do not detect significant absorption at the positions of the Fe II lines at 2382.76, 2586.65 and 2600.17 Å, but these are located in noisier parts of the spectrum. There is also a feature consistent with Mg I 2853 Å at this redshift.

We have remeasured the redshift from the fully calibrated spectrum and find  $z = 0.55185 \pm$

0.00005. To quantify the robustness of this detection we created a mean absorption profile by stacking the positions of the three Mg lines assuming a redshift of  $z = 0.55185$ . The resulting mean profile is shown in velocity space in Fig. 1. There is indeed a fairly clear signal in the mean profile assuming this redshift. The formal significance of the stacked line is  $\sim 7\sigma$ . The two later epochs contain insufficient flux to significantly improve on this estimate. We note that the redshift is consistent with the limit of  $z < 1.5$  reported from *Swift*-UVOT detections in the UVW2 filter (Kuin et al. 2011).

#### 3.2. The first epoch afterglow

Our first epoch afterglow spectrum is well fitted using a simple power-law ( $F_\nu \propto \nu^{-\beta}$ , i.e.  $F_\lambda \propto \lambda^{\beta-2}$ ). Using the UV – optical range, we find  $\beta_{\text{opt}} = 0.92$  (Fig. 2), with systematic errors from the wavelength-dependence of the slit-loss around 10% indicated by the shaded area in the figure. The observed slope is consistent with the X-ray power-law slope measured by the *Swift* X-Ray Telescope (XRT),  $\beta_X = 0.88 \pm 0.09$  (Evans et al. 2009).

Also shown in Fig. 2 are the nearly simultaneous measurements from GROND and those from *Swift*-UVOT, (Kuin et al. 2010; Kuin, private communication). A temporal decay  $F_\lambda \propto t^{-1}$  is adopted to correct for the (small) time difference.

From the X-ray and optical fluxes, we calculate the broad-band spectral index ( $\beta_{\text{OX}}$ ) (see Jakobsson et al. 2004). We find  $\beta_{\text{OX}} = 1.02 \pm 0.10$ , where the error arises from the uncertainty in the spectral index reported in the XRT spectrum and from the choice of the two wavelength points.

The fact that  $\beta_X$ ,  $\beta_{\text{opt}}$  and  $\beta_{\text{OX}}$  are identical

within their uncertainties shows that not only the slopes, but also the normalizations of the optical and X-ray spectra are consistent, hence both components belong to the same power-law segment. This also indicates that little dust can be present along the line of sight (see § 3.4).

### 3.3. Detection of a supernova

In Fig. 3, spectra from all the three epochs are shown together with the first epoch power-law fit. GRB afterglows have power-law spectra, which is seen in the first epoch (as highlighted in Fig. 2). This is clearly not what we observe at later times; in the second epoch spectrum there is a prominent bump at 7800 Å and an increase in flux from 5000 to 5500 Å. The third-epoch spectrum also reveals a bump at  $\sim 8400$  Å.

We have overplotted on the second epoch spectrum a combination of the fading power-law afterglow ( $\sim 20$  times dimmer than in the first epoch) and the spectrum from SN 1998bw (8 day past explosion and corrected for Galactic extinction; Patat et al. 2001) redshifted to  $z = 0.55185$ . We scaled the flux of SN 1998bw by a factor of 1.4 to match our observations from 5000 to 8000 Å. This reproduces fairly well both the bump and the flux increase. Epoch 2 corresponds to 10.6 days in the rest frame of the burst, for which the SN 1998bw spectrum at 8 days is the closest available match with sufficient wavelength coverage. We note that SN 1998bw brightened by about 0.3 mag between 8 and 10.6 days (Galama et al. 1998), hence the flux level is consistent between the two events.

For the third epoch we overplotted a spectrum of SN 1998bw at an epoch of 23 days after the burst in the rest frame. This spectrum of SN 1998bw was chosen to best match the rest-frame epoch for our spectral observations of GRB 101219B and moved to  $z = 0.55185$  with no additional flux scaling. The data are again consistent with the presence of a SN similar to SN 1998bw, although the possible contribution from residual afterglow and from the host galaxy (see § 3.4) limit the scope of this comparison.

We emphasize that in making these comparisons we have made very few assumptions and used few free parameters. The redshift was fixed to that measured from the absorption lines and the afterglow spectral slope is consistent with the X-

ray slope. The SN 1998bw spectra were chosen for epochs dictated by our observations. We attribute the bluest part of the second epoch spectrum to the optical afterglow, since the SN is unlikely to contribute substantially in this regime (due to UV line blanketing, see e.g.; Mazzali et al. 2003). The afterglow is thus  $21 \pm 1$  times fainter than in the first epoch. The only free parameter in the comparison with the epoch 2 spectrum is that we scaled the spectrum of SN 1998bw up by 40% (consistent with the time evolution of SN 1998bw).

The only plausible explanation for the nice match is that an energetic SN was indeed associated with GRB 101219B. We note that Olivares et al. (2011), using GROND, reported photometric evidence for a SN component in their light curves of GRB 101219B with an estimated redshift of  $z \approx 0.4\text{--}0.7$ . Following our discovery, the IAU dubbed this event SN 2010ma (Sparre et al. 2011).

### 3.4. Dust extinction and host galaxy continuum

The fact that our power-law fit agrees with the first epoch spectrum all the way out to the bluest end, and even extrapolates into the UVOT and XRT regimes (Fig. 2), demonstrates that this GRB suffered from negligible extinction. Adding an SMC-like dust extinction when fitting the afterglow did not improve the fit. To put an upper limit to the  $V$ -band absorption  $A_V$ , we fitted the normalization and the spectral slope to a model, where  $A_V$  was fixed to 0.1 mag. In the UVB part of our spectrum this model gave a worse fit than the dust-free fit, and it also did not match the UVOT points, so we conclude that  $A_V < 0.1$  mag. The lack of excess X-ray absorption (Gelbord et al. 2010b) and the weakness of the absorption features (§ 3.5) are consistent with a tenuous host galaxy medium.

From the Gemini images obtained on Jan 29 and Jan 30 we infer the following limits and measurements of the source:  $u > 24.5$ ,  $g = 24.1 \pm 0.2$ ,  $r = 23.7 \pm 0.2$ , and  $i = 23.8 \pm 0.2$ . This corresponds to a monochromatic flux of about  $9 \times 10^{-19}$  erg  $\text{cm}^{-2} \text{s}^{-1} \text{Å}^{-1}$  in the  $r$  band, consistent with the third epoch spectrum. It is not clear if this corresponds to the host galaxy alone or whether there is some contribution from the afterglow or the SN. To test how much such a contribution could affect

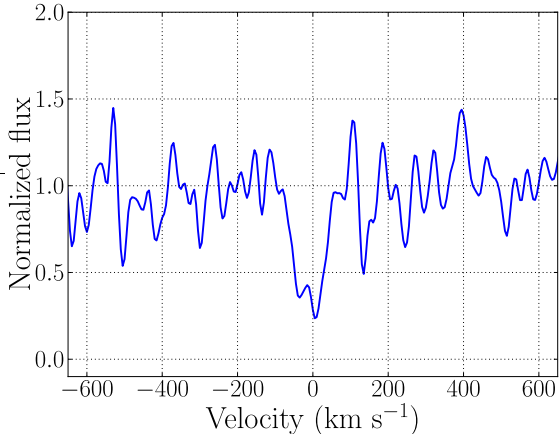


Fig. 1.— The mean velocity profile for the first epoch spectrum, for three Mg absorption lines detected at 4339.6, 4350.7, and 4427.5 Å assuming a redshift of  $z = 0.55185$ . Each line was converted to rest frame vacuum wavelength zero velocity before stacking.

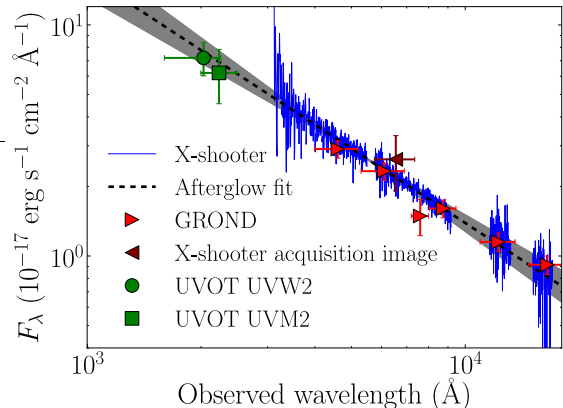


Fig. 2.— The first epoch spectrum, which was taken 11.6 hr after the burst, fitted with a power-law. Also shown are fluxes from imaging with GROND, *Swift*-UVOT, and our own acquisition image. The GROND-fluxes were used to fix the normalization of our spectrum. Regions dominated by atmospheric features and instrumental artifacts are excluded from the plot and from the fit. In the fit we excluded the NIR ( $\lambda > 11,000$  Å), due to a possible systematic error in the offset between the flux-calibrated spectra in the VIS and in the NIR.

the luminosity of the SN in the second epoch, we assumed as an upper limit that the host galaxy has a wavelength-independent flux corresponding to what is measured in the third epoch spectrum. To this value we added a faded afterglow and a contribution from SN 1998bw. In this way, the SN would be 30% fainter than assuming no host contamination. The host galaxy is thus unlikely to affect the conclusion that a luminous SN component is dominating our epoch 2 spectrum.

We have also searched the spectra for the strongest host galaxy emission lines. Unfortunately, at  $z = 0.55185$  [O II]  $\lambda 3727$  and H $\alpha$  fall in the transition regions between the UVB/VIS and VIS/NIR arms, respectively. However, [O III]  $\lambda 5007$  is located in a clear part of the spectrum. To derive an upper limit on the line flux we added artificial emission lines of increasing strength to the data, until the line was easily detectable. For [O III]  $\lambda 5007$  we find that an emission line of  $3 \times 10^{-17}$  erg s $^{-1}$  cm $^{-2}$  would have been detected. At the redshift of the burst this corresponds to a luminosity of  $L_{[\text{O III}]} = 4 \times 10^{40}$  erg s $^{-1}$ . While this limit is not unprecedented (for example, the host galaxy of GRB 030329 has  $L_{[\text{O III}]} = 3 \times 10^{40}$  erg s $^{-1}$ ; Hjorth et al. 2003), this value lies at the lower end of the distribution (Savaglio et al. 2009), consistent with a faint host galaxy.

### 3.5. Mg absorption in the host galaxy

Table 2 displays the equivalent widths of the absorption features in the first epoch spectrum. Mg II  $\lambda 2796$  is stronger than Mg II  $\lambda 2803$  and their ratio ( $1.37 \pm 0.37$ ) is consistent with the average value ( $1.16 \pm 0.03$ ) of the composite spectrum presented by Christensen et al. (2011). These lines are weaker than the ones of the typical GRB spectrum, but similar or even weaker cases have been seen before (e.g., GRB 050922C: Piranomonte et al. 2008; GRB 070125: Fynbo et al. 2009). The detection limits of iron lines are consistent with the weak magnesium features.

## 4. Discussion

In this paper we report on our detection of the spectral signature of a SN, SN 2010ma, in the fading afterglow spectrum of GRB 101219B.

The redshift was measured to be  $z = 0.55185$

based on our detections of weak Mg II absorption lines in the first epoch spectrum. At this redshift, a SN similar to SN 1998bw can well match our second epoch spectrum. The broad spectral features indicate high velocities in the expanding ejecta, whereas a normal SN Ib/c clearly does not match the observations. A SN interpretation is consistent with the drop at  $\sim 5000 \text{ \AA}$  being due to UV blanketing in the SN spectra, where the UV part is instead dominated by the blue afterglow component. The host galaxy appears to be relatively faint, which likely contributed to obtain a clean signal from the supernova. There is little room for host galaxy extinction.

The GRB itself is clearly of long duration and has, at the measured redshift, an isotropic equivalent energy of  $4.2 \times 10^{51}$  erg. It has a bright afterglow with a standard light curve, and obeys the  $E_p$ - $E_{\text{iso}}$  (“Amati”) relation (Amati et al. 2007). It is thus fully representative of the high-luminosity, routinely observed high-redshift population of GRBs, for which we now can provide a robust, spectroscopic association with a SN.

Since 4 out of the 5 previously unambiguously spectroscopically confirmed SN-GRBs were in fact rather low luminosity bursts with unusual afterglows and spectral properties, there have been suggestions in the literature (e.g., Kaneko et al. 2007) that the GRB-SN association is only proven for the local universe. Our new association favours a GRB-SN connection also for the main population of cosmological GRBs. This confirms previous observations of photometric bumps and tentative spectroscopic SN detections for distant bursts. In the recent compilation by Hjorth & Bloom (2011), the evidence for the SN association of GRB 101219B was graded just after the five ‘ironclad’ cases mentioned in § 1. The fact that we were able

Table 2: Equivalent widths for the absorption features in the first epoch spectrum, both in the observer and rest frames. Limits are at  $3\sigma$ .

Feature	$EW_{\text{obs}} (\text{\AA})$	$EW_{\text{rest}} (\text{\AA})$
Fe II $\lambda 2586$	$<0.96$	$<0.62$
Fe II $\lambda 2600$	$<0.90$	$<0.58$
Mg II $\lambda 2796$	$1.34 \pm 0.25$	$0.86 \pm 0.16$
Mg II $\lambda 2803$	$0.98 \pm 0.20$	$0.63 \pm 0.13$
Mg I $\lambda 2852$	$0.89 \pm 0.18$	$0.57 \pm 0.12$

to see the SN component emerge over three epochs with the same instrumentation leaves little room for confusion by afterglow or host galaxy emission — also thanks to the faintness of the host. The X-shooter spectrograph will with no doubt continue to contribute to this area of research.

## Acknowledgements

We acknowledge Michael Andersen, Massimo Della Valle, Suzanne Foley, Paul Kuin, and Paul Vreeswijk for helpful comments. The Dark Cosmology Centre is funded by the Danish National Research Foundation. GL is supported by a grant from the Carlsberg foundation. RAMJW acknowledges support from the European Research Council via Advanced Investigator Grant no. 247295. SS acknowledges support by a Grant of Excellence from the Icelandic Research Fund.

## REFERENCES

- Amati, L., Della Valle, M., Frontera, F., Malesani, D., Guidorzi, C., Montanari, E., & Pian, E. 2007, *A&A*, 463, 913
- Bufano, F., Benetti, S., Sollerman, J., Pian, E., & Cupani, G. 2011, *Astronomische Nachrichten*, 332, 262
- Cano, Z., et al. 2011, *ArXiv*: 1104.5141C
- Cano, Z., et al. 2011, *MNRAS*, 413, 669
- Cardelli, J. A., Clayton, G. C., & Mathis, J. S. 1989, *ApJ*, 345, 245
- Chornock, R., et al. 2010, *arXiv*:1004.2262
- Christensen, L., Fynbo, J. P. U., Prochaska, J. X., Thöne, C. C., de Ugarte Postigo, A., & Jakobsson, P. 2011, *ApJ*, 727, 73
- Cummings, J. R., et al. 2010, *GRB Coordinates Network*, 11475
- de Ugarte Postigo, A., et al. 2011, *GRB Coordinates Network*, 11579
- Della Valle, M., et al. 2008, *Central Bureau Electronic Telegrams*, 1602, 1
- . 2003, *A&A*, 406, L33
- . 2006, *ApJ*, 642, L103

- D’Odorico, S., et al. 2006, in Presented at the Society of Photo-Optical Instrumentation Engineers (SPIE) Conference, Vol. 6269, Society of Photo-Optical Instrumentation Engineers (SPIE) Conference Series
- Evans, P. A., et al. 2009, *MNRAS*, 397, 1177
- Fynbo, J. P. U., et al. 2009, *ApJS*, 185, 526
- . 2004, *ApJ*, 609, 962
- Galama, T. J., et al. 1998, *Nature*, 395, 670
- Garnavich, P. M., et al. 2003, *ApJ*, 582, 924
- Gelbord, J., et al. 2010a, GRB Coordinates Network, 11473
- . 2010b, GRB Coordinates Network, 11481
- Goldoni, P., Royer, F., François, P., Horrobin, M., Blanc, G., Vernet, J., Modigliani, A., & Larsen, J. 2006, in Presented at the Society of Photo-Optical Instrumentation Engineers (SPIE) Conference, Vol. 6269, Society of Photo-Optical Instrumentation Engineers (SPIE) Conference Series
- Hamuy, M., et al. 1993, *AJ*, 106, 2392
- Hjorth, J., & Bloom, J. S. 2011, ArXiv e-prints astro-ph/1104.2274
- Hjorth, J., et al. 2003, *Nature*, 423, 847
- Jakobsson, P., Hjorth, J., Fynbo, J. P. U., Watson, D., Pedersen, K., Björnsson, G., & Gorosabel, J. 2004, *ApJ*, 617, L21
- Kaneko, Y., et al. 2007, *ApJ*, 654, 385
- Kouveliotou, C., Meegan, C. A., Fishman, G. J., Bhat, N. P., Briggs, M. S., Koshut, T. M., Paciesas, W. S., & Pendleton, G. N. 1993, *ApJ*, 413, L101
- Kuin, N., et al. 2010, GRB Coordinates Network, 11482
- Kuin, N., et al. 2011, GRB Coordinates Network, 11516
- Malesani, D., et al. 2004, *ApJ*, 609, L5
- Mazzali, P. A., et al. 2003, *ApJ*, 599, L95
- Modigliani, A., et al. 2010, in Society of Photo-Optical Instrumentation Engineers (SPIE) Conference Series, Vol. 7737, Society of Photo-Optical Instrumentation Engineers (SPIE) Conference Series
- Nysewander, M., Fruchter, A. S., & Pe’er, A. 2009, *ApJ*, 701, 824
- Olivares, F., et al. 2010, GRB Coordinates Network, 11478
- . 2011, GRB Coordinates Network, 11578
- Patat, F., et al. 2001, *ApJ*, 555, 900
- Pian, E., et al. 2006, *Nature*, 442, 1011
- Piranomonte, S., et al. 2008, *A&A*, 492, 775
- Savaglio, S., Glazebrook, K., & Le Borgne, D. 2009, *ApJ*, 691, 182
- Schlegel, D. J., Finkbeiner, D. P., & Davis, M. 1998, *ApJ*, 500, 525
- Sollerman, J., et al. 2006, *A&A*, 454, 503
- Sparre, M., Fynbo, J., de Ugarte Postigo, A., Malesani, D., & Sollerman, J. 2011, Central Bureau Electronic Telegrams, 2706, 1
- Stanek, K. Z., et al. 2003, *ApJ*, 591, L17
- Starling, R. L. C., et al. 2011, *MNRAS*, 411, 2792
- Tanvir, N. R., et al. 2010, *ApJ*, 725, 625
- van der Horst, A., et al. 2010, GRB Coordinates Network, 11477
- Vernet, J., et al. 2010, in Society of Photo-Optical Instrumentation Engineers (SPIE) Conference Series, Vol. 7735, Society of Photo-Optical Instrumentation Engineers (SPIE) Conference Series
- Woodsley, S. E., & Bloom, J. S. 2006, *ARA&A*, 44, 507
- Zeh, A., Klose, S., & Hartmann, D. H. 2004, *ApJ*, 609, 952

---

This 2-column preprint was prepared with the AAS L<sup>A</sup>T<sub>E</sub>X macros v5.2.

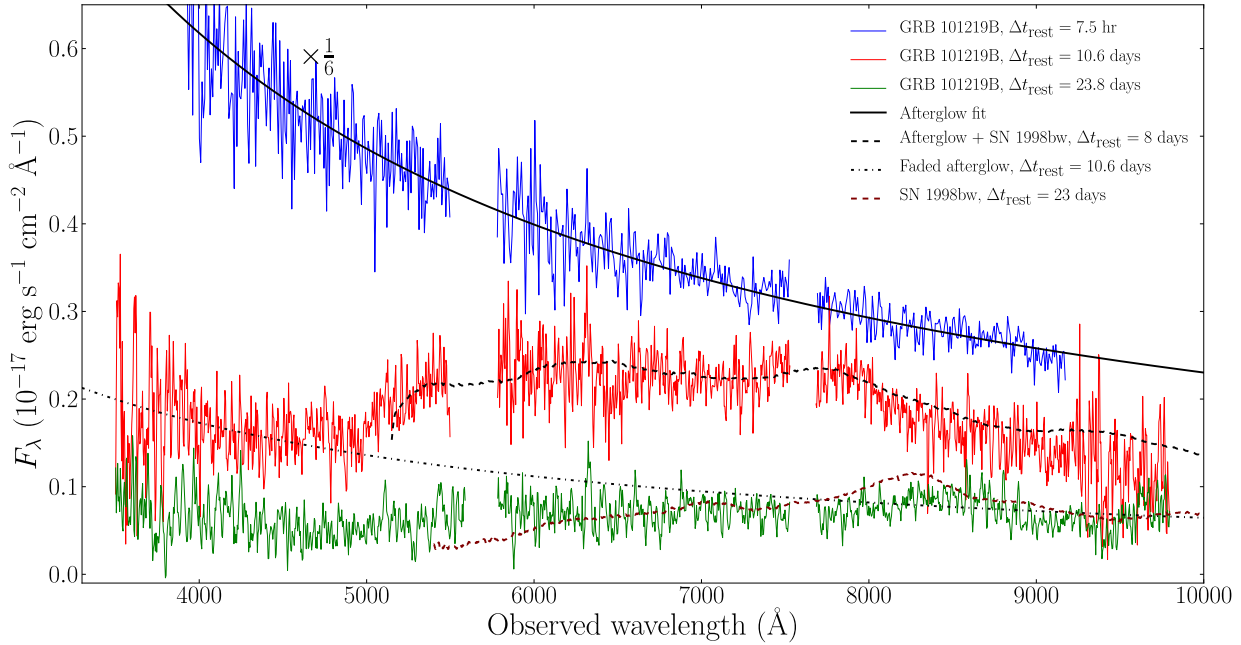


Fig. 3.— Three epochs of spectral observations. The second epoch is compared with a faded afterglow component and the flux from SN 1998bw (8 days after the explosion), multiplied by 1.4. In the third epoch the contributions from the faded afterglow and possible host galaxies are ignored, and the observations are compared to SN 1998bw alone. The flux of the first epoch has been divided by 6 for presentation purposes. The NIR spectra are not shown, because of their low signal-to-noise ratio in the second and the third epoch. Regions dominated by atmospheric and instrumental features are removed from the plot. The spectra are rebinned to a resolution of  $0.8 \text{ \AA}$ .